Fracture Toughness of HSLA Coiled Tubing Used in Oil Wells Operations

J. Wainstein

J. Perez Ipiña

GMF-LPM,
Univ. Nac. del Comahue-CONICET,
Bs. As. 1400, Neuquén, Argentina

Coiled Tubings are thin walled steel tubes of 25–89 mm diameter and thousands meters long, used in the oil industry for production and maintenance services. They suffer plastic deformation during unwinding of the reel, passing through a goosneck arch guide and an injector unit. Strain levels are of 2–3%, making the tubing fail by low cycle fatigue in around 100 wrap–unwrap cycles. As coiled tubing material generally behaves in a ductile manner at surface and down well temperatures, the R *curve has to be known to make instability analyses.* J-R *curves were determined to characterize the fracture toughness of nonused coiled tubing, using nonstandard specimens due to difficulties with their small thickness and diameters. Different crack lengths and crack locations were tested to analyze the* $2C_0/W$ *ratio and the influence of the longitudinal weld. The* R *curves obtained show crack arc length dependence and are influenced by the position of the longitudinal weld.* [DOI: 10.1115/1.4004569]

Keywords: fracture toughness, coiled tubing, oil services, J-R curves

1 Introduction

Coiled Tubings are thin walled steel tubes of 25–89 mm in diameter and several thousands meters long. It is used in oil and energy industries to provide a number of production tasks and maintenance services.

Coiled Tubing is manufactured from longitudinally welded strips. A series of rolls bends the edges of the strip upward gradually forming an U shape. A new series of rolls, having vertical tungsten carbide fins, extend down the strip edges. These fins prepare the strip edges for the weld rolls. The longitudinal weld is made by using the high frequency induction electrical resistance method. A special set of insulated rolls squeeze the edges together while they are at fusion temperature to produce the weld. No filler material is added in the welding operation keeping the metal composition of the weld line the same as the body of the tube. Tubing is welded slightly oversize. The weld seam is immediately reheated by a narrow induction head to recrystalize the weld's heat affected zone to match the grain structure of the base metal. After welding, the tube is cooled before entering the sizing section of the mill, where another set of rolls in pairs accurately form the tubing to its final dimensions [1]. As the length of the coiled tubing is larger than the strip's one, strips are welded together by a computer-aided welding machines, before making the forming and the longitudinal welding, and after a careful preparation of the strips extremes cut at a fixed angle.

Then coiled tubing is wrapped around a 3–5 m diameter reel. In service it is transported to different wells, unwrapped into the bore without disturbing the existing equipment. When servicing is complete, the coiled tubing is retrieved from the well and spooled back onto its reel for transport to the next work location [2].

Coiled tubing suffers plastic deformation during the service process: unwinding out the reel, pass through the *goosneck* arch guide and pass through the injector unit, shown in Fig. 1. Strain levels are approximately 2–3%, making coiled tubing work in elastic plastic regime.

The most dominant factors controlling the deformation behavior of a coiled tubing are the bending/straightening cycles associated with the spool and gooseneck. Such deformation levels, together with internal pressure, makes coiled tubing fail in around 100 wrap and unwrap cycles.

Coiled Tubing typical failure mode is low cycle fatigue [3]. In service operation, a crack initiates at the inner surface of the tube [2,3], it can grow through the thickness, until it reaches the outer surface. Generally, the crack attains the outer surface before the critical condition, leaking instead of breaking, and becoming a through wall thickness crack. As this occurs generally out of the well, the leakage is detected and the tube is taken out of service or repaired. If the leakage occurs inside the well or the tube is not pressurized, the crack can be undetected, and can grow subcritically before attaining a critical length and producing unstable crack growth. In this situation, catastrophically fracture, operators' lives are in risk due to the elastic energy stored in the tubing and also the tubing falls inside the well interrupting its normal function. The well becomes useless until the fractured tubing is "fished" and removed from the well, generating huge economic losses.

It is important to remark that high strength low alloy (HSLA) coiled tubing material generally behaves in a ductile manner at surface and down well temperatures. Hence, the failure occurs by ductile tearing, making necessary to know the *R* curve to make an instability analysis.

To characterize the fracture toughness of the unused *coiled tubing J-R* curves were determined. Over the years, materials *J-R* curves have been evaluated by conducting tests on compact tension and three point bending specimens according to, for example, ASTM E-1820 [4]. But *coiled tubing* present experimental difficulties for this type of specimen construction, because of its low thickness and small diameter. To overcome this problem, specimens were made with coiled tubing pieces. Because the specimens were not standard, the test was carried out adapting Chattopadhyay et al. [5] tubes test to the coiled tubing dimensions. The evaluation of *J*-integral from test data was made by the recently derived limit load analyses developed by Chattopadhyay et al., based on expressions of η_{pl} and γ functions.

The aim of this paper is to analyze the effect of crack arc length to width (perimeter) ratio (2C/W) and the influence of the longitudinal weld on coiled tubing *J-R* curves. For this purpose *non* standard methodology used by Chattopadhyay et al. [5] was adapted to determine coiled tubing *J-R* curves using non standard specimens.

Contributed by the Pressure Vessel and Piping Division of ASME for publication in the JOURNAL OF PRESSURE VESSEL TECHNOLOGY. Manuscript received June 5, 2010; final manuscript received April 28, 2011; published online December 20, 2011. Assoc. Editor: F. W. Brust.

 Copyright © 2012 by ASME

Downloaded 09 May 2012 to 130.207.50.37. Redistribution subject to ASME license or copyright; see http://www.asme.org/terms/Terms_Use.cfm

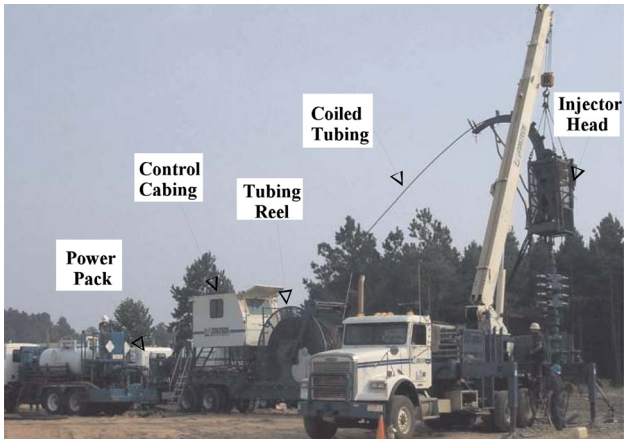

Fig. 1 Coiled tubing unit in service

2 Materials and Experimental Procedure

2.1 Test Specimens. Test specimens were cut-out from two "unused" coiled tubing, meaning that the tubes were not used in well services. The tubes were provided by San Antonio International Company. Due to geometrical difficulties about coiled tubing thickness and diameter, test specimens consisted of coiled tubing segments, of 1 m long, with a through wall circumferential crack, machined by a milling machining process and then fatigue precracked. Figure 2 shows the geometry of the specimens.

Different crack arc lengths were machined in order to evaluate the $2C_0/W$ ratio effect on the *J-R* curves, where $2C_0$ is the initial arc crack length and W is the tube perimeter.

To analyze the longitudinal weld influence on *J-R* curves, two different crack locations with reference to the longitudinal weld were prepared in both tubes, as shown in Fig. 3. Specimens with a crack location opposite to the weld were called coiled tubing A (CTA), and the ones with a crack location next to the weld were called coiled tubing B (CTB).

2.2 Test Arrangements. Because specimens were not standard, the test was carried out adapting Chattopadhyay tubes test [5] to coiled tubing dimensions.

All specimens were subjected to four point bending loading in a Wolpert Universal Testing Machine at room temperature. The specimens were fatigue precracked. (2–10 mm at each side) before performing the fracture tests. This ensured a sharp crack tip. The geometric details of the tested specimens are given in Table 1.

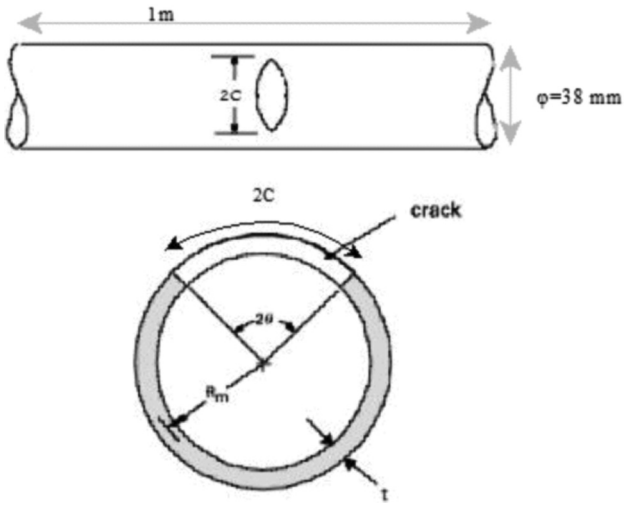

Fig. 2 Geometry of a tube with a circumferential through wall crack

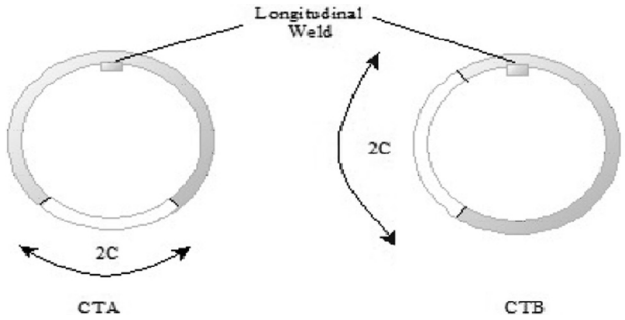

Fig. 3 Crack location with respect to longitudinal welding

2.3 Instrumentation and Data Acquisition. Applied load and load line displacements were directly measured during the tests, while the crack arc growth (2C) was measured by the direct current potential drop (DCPD) method. The DCPD method represents one of the methods used to measure crack length during fracture mechanics testing. It was implemented because it only requires a conductor material and it is suitable to use with no standard specimens. Advantages and problems related to the application of DCPD method were discussed in Refs. [6, 7]. Problems like high-capacity current sources or the necessity to insulate the specimen, are mostly negligible in laboratory conditions. In the other hand, it has advantages as stability, reproducibility, and insensitivity to movement of cables. In any case, the DCPD measurement is one of the most reliable and convenient methods monitoring of crack growth process, with no need for direct time consuming optical measurements [8–10]. It requires a calibration curve which relates crack arc length with the corresponding potential drop. This curve was determined using several coiled tubing specimens, with different crack arc lengths; 20 A current was applied to coiled tubing specimens. The potential drop was measured for every stationary crack arc length.

After testing, specimens were heat tinted and then cooled for broken in order to observe the fracture surface. The initial and final crack arc lengths were measured on the fracture surface.

2.4 Analysis Procedure. The evaluation of *J*-integral from test data was made and derived by Chattopadhayay et al. [5] recently, limit load analyses that are based on expressions of η_{pl} and γ functions. The great advantage of these general expressions is that η_{pl} and γ can be very easily determined for any crack geometry, because limit load expressions of most of the crack components of general interest are easily available in literature [11]. Hence, for the particular case of four point bend tubings, the expressions employed to calculate the *J* values were taken from Refs. [5, 12–14]. The *J*-integral of through wall circumferential cracked pipe under bending can be expressed as:

$$J = J_e + J_p \tag{1}$$

$$J_e = K^2/E \tag{2}$$

$$J_p = J_{p0} + \int_{\theta 0}^{\theta} \gamma J_{p0} d\theta \tag{3}$$

where

$$J_{po} = \int_0^{\Delta p} \beta \cdot P d\Delta_p \tag{4}$$

$$\beta = h_1/[(2-\zeta)tR_0h] \tag{5}$$

$$h = [\cos(\theta/2) - 0.5\sin\theta] \tag{6}$$

$$h_1 = 0.5[\sin(\theta/2) + \cos\theta] \tag{7}$$

$$\varsigma = t/R_0 \tag{8}$$

Downloaded 09 May 2012 to 130.207.50.37. Redistribution subject to ASME license or copyright; see http://www.asme.org/terms/Terms_Use.cfm

Table 1 Details of test specimen

Tube	Specimens	Outside diameter (mm)	Wall thickness (mm)	Span (mm)		Initial are length (mm)	Angle (θ_0)
				Smaller	Higger		
Tube 1	CTA-1	38.1	3.20	275	700	36.5	52.1
	CTA-2	38.2	3.25	275	700	57.8	86.7
	CTA-3	38.3	3.25	275	700	55.7	83.3
	CTB-1	38.3	3.20	275	700	41.2	61.6
	CTB-2	38.2	3.22	275	700	40.0	60.0
	CTB-3	38.3	3.25	275	700	41.3	61.7
Tube 2	CTA-4	38.2	3.25	275	700	59.8	93.5
	CTA-5	38.2	3.25	275	700	54.3	82.6
	CTA-6	38.3	3.30	275	700	67.2	100.7
	CTA-7	38.2	3.24	275	700	73.2	109.6
	CTB-4	38.2	3.25	275	700	55.3	82.7
	CTB-5	38.2	3.20	275	700	48.1	68.9

$$\gamma = [0.5\cos(\theta/2) - \sin\theta]/[\sin(\theta/2) + \cos\theta] \quad (9)$$

$$\theta = \theta_0 + d\theta \quad (10)$$

where Δ_p is the plastic component of the load point displacement due to the crack, R_o and t are the pipe outer radius and wall thickness, respectively, P is the applied central load under four point bending, θ_o and θ are the initial and current crack half angle, respectively, and $d\theta$ is the crack growth at each crack tip.

3 Results and Discussion

In service operating coiled tubing a circumferential crack generally initiates at the inner surface of the tube. Then the crack can grow through the thickness. Two possibilities may arise in this situation:

(a) Sudden rupture may take place before the crack reaches the surface, causing a break before leak condition. In this case, the crack growing through the thickness, reaches its critical crack size. It must be taken into account that the critical crack size could be changing in every tensile strain cycle [2].
(b) The crack can grow through the thickness until it reaches the outer surface and attains a leak before break condition. It becomes a through wall thickness crack. In case the tube is not repaired or taken out of service, subcritical crack growth may occur after this condition, until a critical crack size is reached, and the total failure occurs.

Although both cases (a) and (b) can occur in service operation, according to the experience related by users, in most operation conditions case (b) takes place. At the outside and inside well temperatures, the tube material works in the upper shelf in which the failure mode can be by ductile tearing. In this situation, the material R curve is necessary to make an instability analysis.

Fracture tests were carried out on through wall cracked coiled tubing. The crack growth during the test was measured by the DCPD method [8–10]. The calibration curve obtained is shown in Fig. 4. The potential drop measured was normalized with the current density in order to be independent of the coiled tubing diameter.

Once the potential drop calibration curve was determined, fracture tests were conducted.

Figure 5 shows the load versus load-point-displacement records for various coiled tubing obtained during the fracture toughness tests. Initial crack arc length ($2C_0$), varied from 36 to 73 mm.

Figure 6 shows crack extension versus displacement determined from the measured DCPD.

This figure also shows the initial and final crack lengths measured on the fracture surface of each specimen, which were used as reference values. A photograph of a fracture surface is shown in Fig. 7.

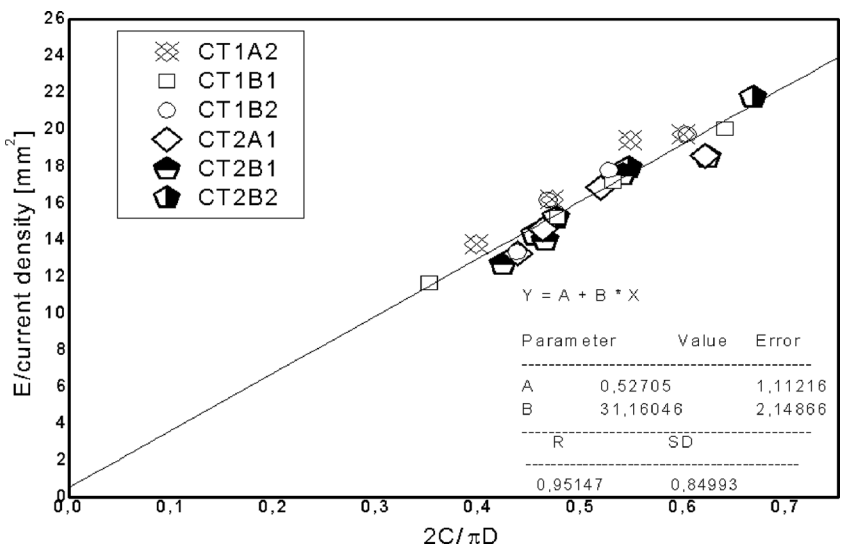

Fig. 4 Potential drop versus normalized arc length

Downloaded 09 May 2012 to 130.207.50.37. Redistribution subject to ASME license or copyright; see http://www.asme.org/terms/Terms_Use.cfm

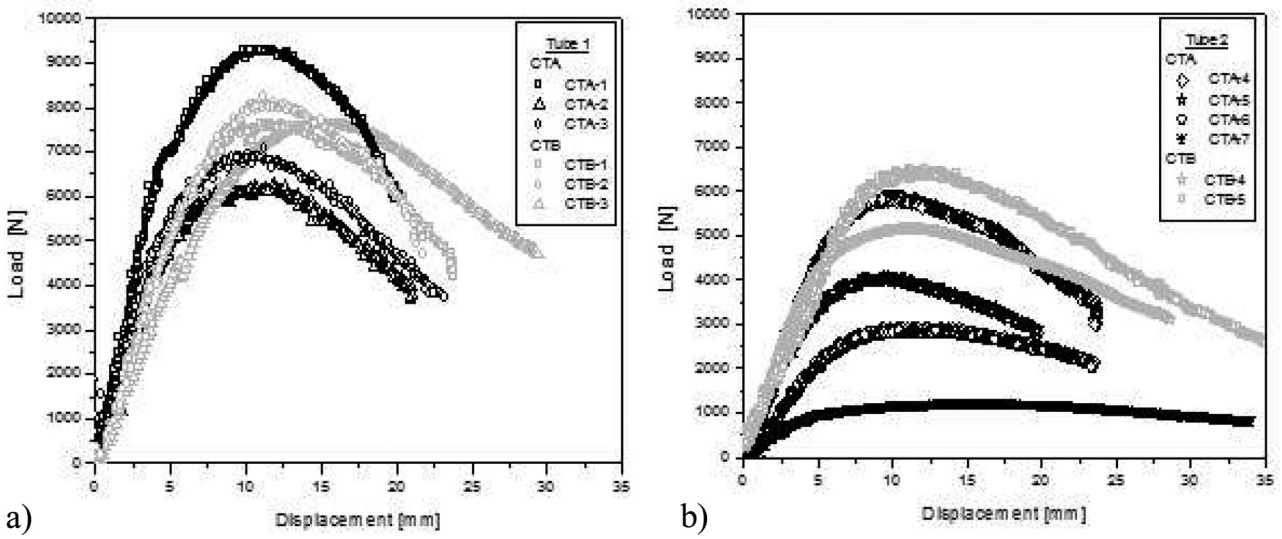

Fig. 5 Load versus load line displacement records for coiled tubing (*a*) tube 1 and (*b*) tube 2

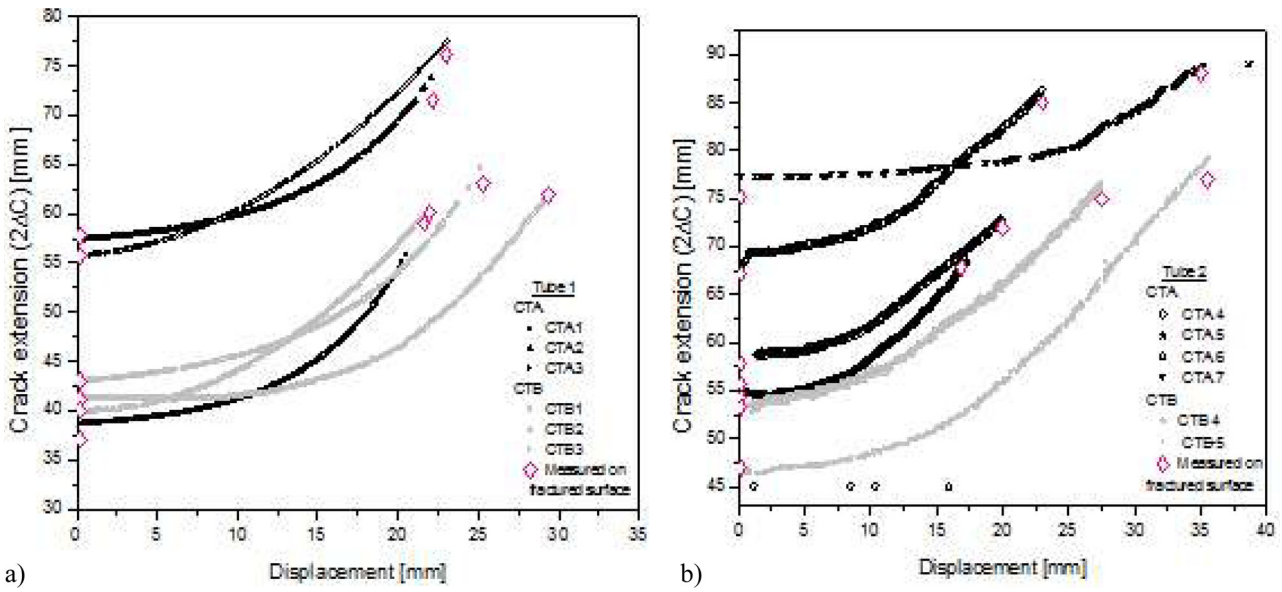

Fig. 6 Crack extension (2ΔC) versus displacement records. (*a*) Tube 1 and (*b*) tube 2.

As already mentioned, crack extension was determined as an arc length. The initial crack arc length measured on the fracture surface is pointed on the photograph as machined notch plus fatigue precrack. The final arc crack length includes the machined notch, the fatigue precrack and the stable crack growth on both sides. Table 2 shows the differences between the crack growths obtained by the potential drop method and by direct measurement on the tube fracture surfaces. They were smaller than 10% in all the cases.

In order to determine *J-R* curves, load displacement data were reduced to obtain plastic displacement as follows: First, the actual compliance was calculated from the initial slopes of the load displacements curves then the elastic displacement was subtracted from the total displacement, using the compliance measured from the test records, in order to obtain the plastic displacements as follows:

$$\nu_{pl} = \nu - P \cdot C$$

Fig. 7 Fracture surface macrograph

Downloaded 09 May 2012 to 130.207.50.37. Redistribution subject to ASME license or copyright; see http://www.asme.org/terms/Terms_Use.cfm

Table 2 Crack growth comparison between fracture surface measurements and those calculated from the potential drop method

Tubes	Specimen	Crack growth measured on fracture surface (mm)	Crack growth obtained by potential drop (mm)	2ΔC differences (%)
Tube 1	CTA-1	15.2	16.1	5.90
	CTA-2	14.2	13.5	4.92
	CTA-3	16.0	16.3	1.85
	CTB-1	16.1	16.4	1.90
	CTB-2	15.9	15.8	0.62
	CTB-3	19.3	20.5	6.21
Tube 2	CTA-4	14.1	14.7	4.25
	CTA-5	12.9	13.5	4.65
	CTA-6	14.7	15.6	6.12
	CTA-7	11.2	11.4	1.78
	CTB-4	20.5	21.4	4.40
	CTB-5	24.5	24.7	0.81

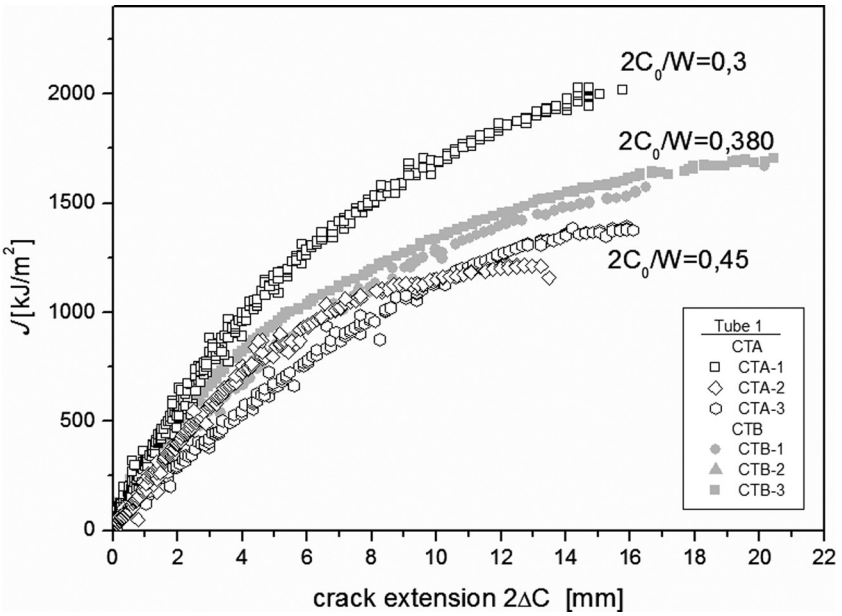

Fig. 8 *J-R* curve for coiled tubing, tube 1

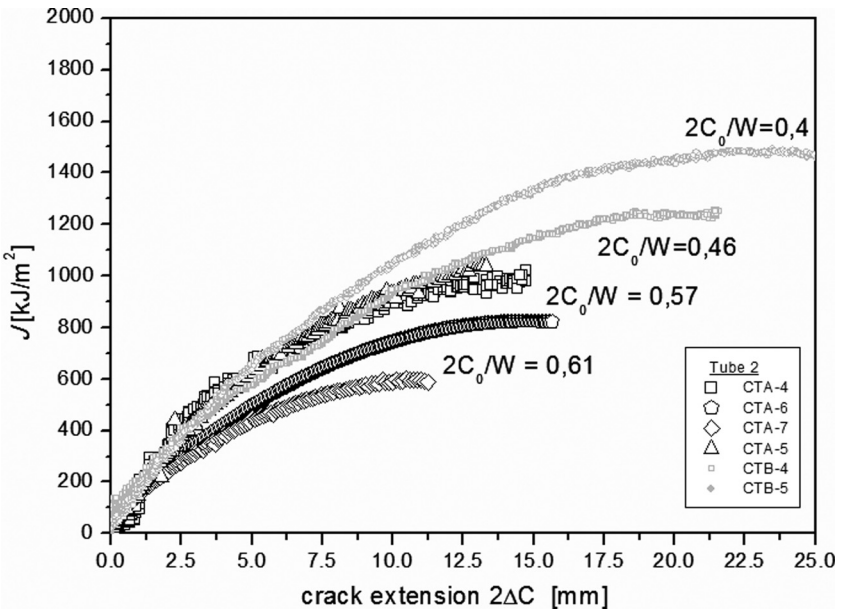

Fig. 9 *J-R* curve for coiled tubing, tube 2

Downloaded 09 May 2012 to 130.207.50.37. Redistribution subject to ASME license or copyright; see http://www.asme.org/terms/Terms_Use.cfm

Table 3 J_{IQ}, J_{max}, and $2\Delta C_{max}$ (ASTM E1820-08)

Specimens		$2C_0$ (mm)	$W = 2\Pi R$ (mm)	$2C_0/W$	b_0 (mm)	ASTM E-1820 (*) J_{IQ} (kJ/m^2)	ASTM E-1820 (*) $2\Delta C_{max} = 0.25*b_0$ (mm)	ASTM E-1820 (*) $J_{max} = B*\sigma_y/10$ (kJ/m^2)
Tube 1	CTA-1	36.5	119.7	0.30	83.2	130	20.8	184.1
	CTA-2	57.8	120.0	0.48	62.2	109	15.5	184.1
	CTA-3	55.7	120.3	0.46	64.6	141	16.1	184.1
	CTB-1	41.2	120.3	0.34	79.1	114	19.7	157.8
	CTB-2	40.0	120.0	0.33	80.0	125	20.0	157.8
	CTB-3	41.2	120.3	0.34	79.0	144	19.7	163.0
Tube 2	CTA-4	59.8	120.0	0.46	64.2	125	16.0	173.5
	CTA-5	54.3	120.0	0.45	65.7	118	16.4	178.8
	CTA-6	67.2	120.3	0.56	53.1	120	13.3	173.5
	CTA-7	73.2	120.0	0.61	46.8	90	11.7	175.6
	CTB-4	55.3	120.0	0.46	64.7	117	16.2	175.6
	CTB-5	48.1	120.0	0.40	71.9	127	17.9	173.5

Figures 8 and 9 show the *J-R* curves of coiled tubing before they were used in wells, determined by Eqs. (1)–(10) described in Sec. 2.4.

Table 3 shows the limits in J_{max} and D2*C* established in ASTM-E1820-08. For the tested coiled tubings, $J_{max} = B\sigma_y/10 = 184.1\ kJ/m^2$ resulted much smaller than the applied *J* values.

Therefore, these curves are valid only for the current evaluated conditions since either the relative crack length or tubing thickness or both are not large enough to assure proper dimensions for *J*-controlled stable crack growth under high-constraint conditions [4].

As it can be seen on Figs. 8 and 9, *J-R* curves of *coiled tubing*, vary with the $2C_0/W$ ratio. Initial arc crack lengths varied from 36 mm to 73 mm hence $2C_0/W$ varied from 0.30 to 0.61. The differences on the *J-R* curve slopes could be related to in plane constraint dependence [15,16]. Figures 8 and 9 also shows that the bigger $2C_0/W$, the lower the curve is. Figure 10 shows fracture surfaces of tested coiled tubing. On CTB-3 it is remarkable that the stable crack growth produced a significant thickness reduction. The thickness reductions of all specimens are quantified in Table 4. It is noticeable that the longer the crack growth, the bigger the thickness reduction was, probably because out of plane constraint reduction [17].

On the other hand, CTBs have initial arc crack location close to the longitudinal weld, as shown in Fig. 3. Crack growth on these specimens was halted by the longitudinal weld bead, indicated with white arrows on Fig. 10.

In these situations, the longitudinal weld acted as a barrier to the crack growth, evidenced by a greater growth on the opposite side—indicated with light gray arrows—in Fig. 10-CTB-3. *J-R* curves of CTBs specimens seem to be higher than the ones of similar initial arc crack length located opposite to the weld bead,

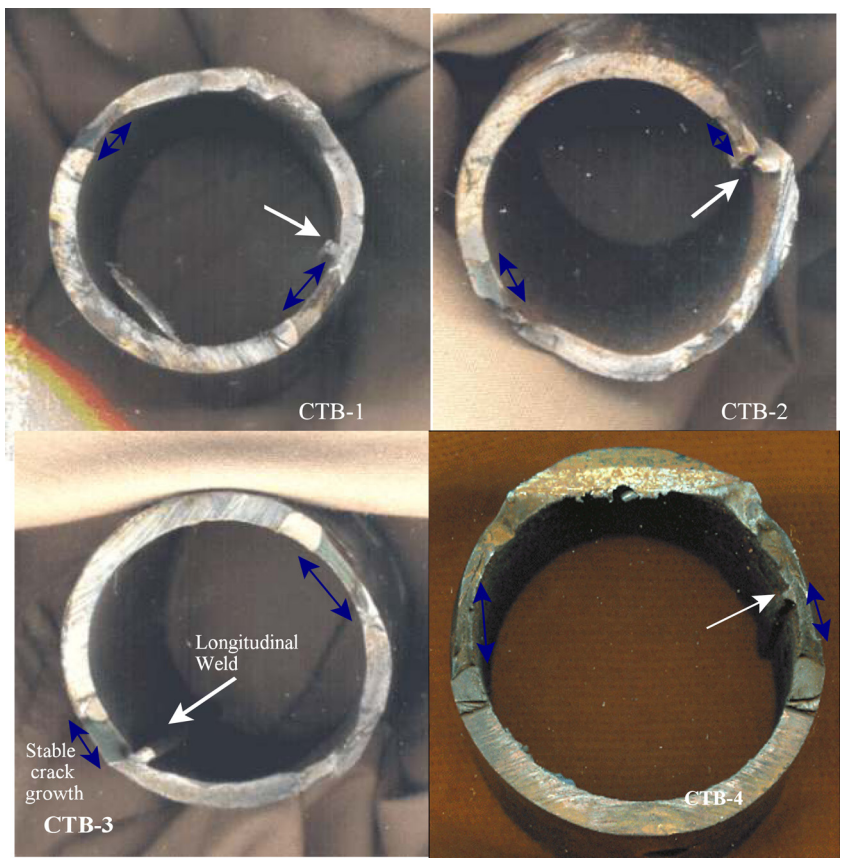

Fig. 10 Fracture surfaces of four of the tested coiled tubing

Downloaded 09 May 2012 to 130.207.50.37. Redistribution subject to ASME license or copyright; see http://www.asme.org/terms/Terms_Use.cfm

Table 4 Out of plane constraint

Tubes	Specimen	Crack growth measured on fracture surface (mm)	Wall thickness (mm)	Wall thickness decrease (mm)	Wall thickness decrease (%)
Tube 1	CTA-1	15.2	3.20	0.53	16.5
	CTA-2	14.2	3.25	0.45	13.8
	CTA-3	16.0	3.25	0.45	13.8
	CTB-1	16.1	3.20	0.50	15.6
	CTB-2	15.9	3.22	0.57	11.1
	CTB-3	19.3	3.25	0.65	20.0
Tube 2	CTA-4	14.1	3.25	0.50	15.3
	CTA-5	12.9	3.25	0.54	16.6
	CTA-6	14.7	3.30	0.55	16.6
	CTA-7	11.2	3.24	0.34	10.5
	CTB-4	20.5	3.25	1.35	41.5
	CTB-5	24.5	3.20	1.22	38.1

CTAs. The longitudinal weld seems to contribute to increase the apparent material *J-R* curve, as shown in Fig. 11.

When the stable crack growth pass through the longitudinal weld (as in Fig. 12, picture number 2, CTB-4), it would be reasonable to think that the crack experiences the increase in the thickness on that crack tip, as the local phenomena, resulting in the decrease on the effective driving force.

The amount of crack growth in that tip would be smaller, as Fig. 12 shows. But, in global terms and considering a constant thickness for *J* calculation, the acting *J* should be the same on

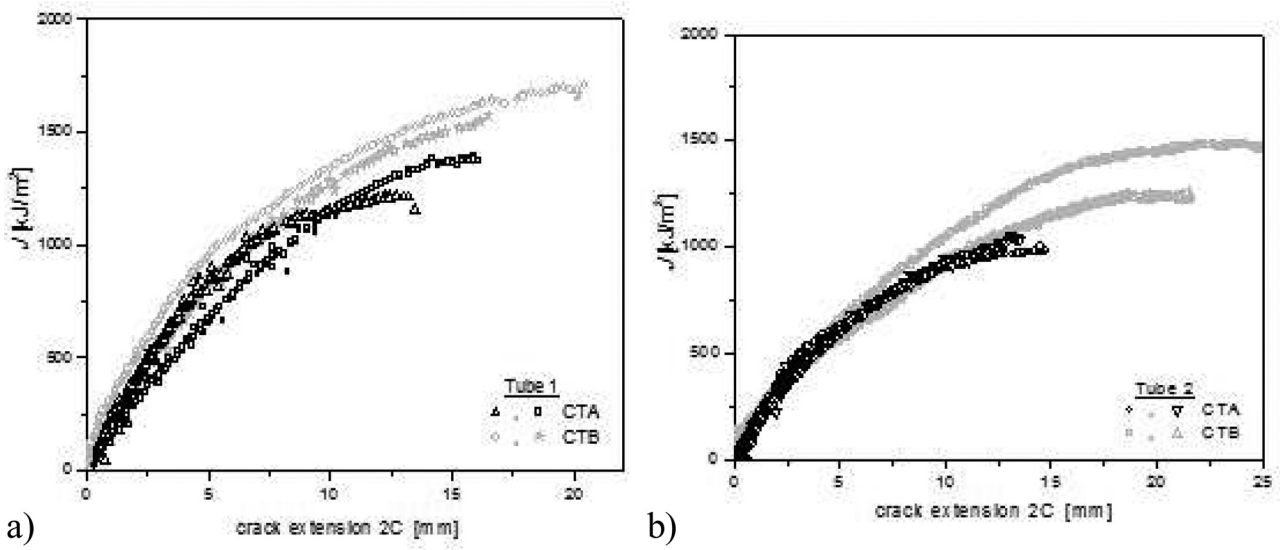

Fig. 11 *J-R* curves CTAs and CTBs (*a*) tube 1 and (*b*) tube 2

Fig. 12 Stable crack growth through the longitudinal weld

Downloaded 09 May 2012 to 130.207.50.37. Redistribution subject to ASME license or copyright; see http://www.asme.org/terms/Terms_Use.cfm

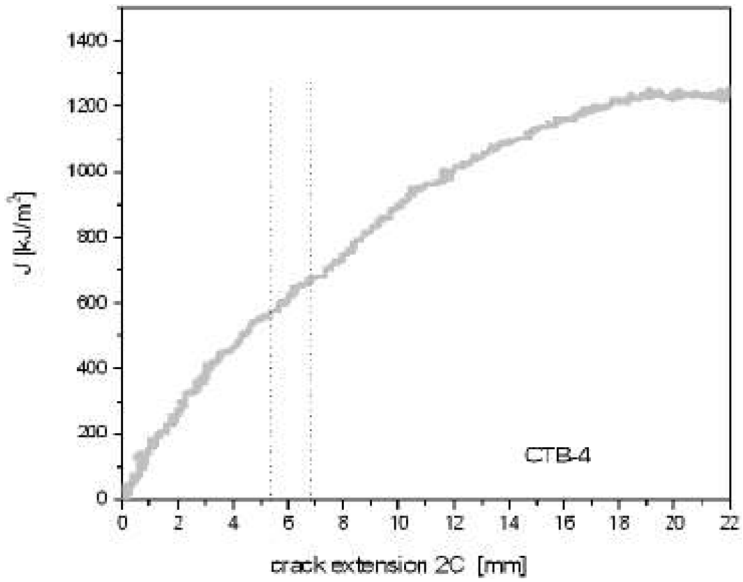

Fig. 13 CTB-4 *J-R* curve

both the extremes of the crack. Therefore, if we analyze the *R* curve as global phenomena, this decrease in the effective driving force could result in a step on the *J-R* curve. This step could be attenuated because thickness increase due to the longitudinal weld also induced an increase on the local constraint. Hence, it would be a competition between both the local phenomena, a decrease in effective driving force, and an increase on local constraint, generally occurring the first one. Figures 13 and 14 show CTB-4 and CTB-5 *R* curves, both present a slightly slope change between two vertically straight lines, which are pointing the length from the initial arc crack length, to the beginning and end of the longitudinal weld, measured on the fracture surfaces.

It could be seen that the longitudinal weld affects the *J-R* curve, making the material component beside the longitudinal weld more resistant to crack growth.

An instability analyses has been performed to characterize the toughness of coiled tubing ductile material during stable crack growth. At the outside and inside well temperatures, the tube material works in the upper shelf in which the failure mode can be by ductile tearing. In this situation, all the *R* curve is important to make an instability analysis. The J_{IC} values are listed but they are related to the crack growth beginning, and they are considered to be conservative for an estructure which can attain some stable crack growth without compromising its integrity. The present work is a first step in the instability analysis of coiled tubing. On going work on this analysis is already in progress.

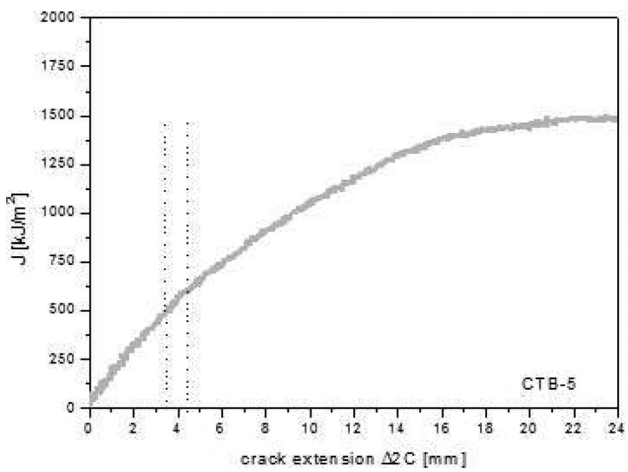

Fig. 14 CTB-5 *J-R* curve

4 Summary and Conclusions

J-R curves were determined using nonstandard specimens to characterize the fracture toughness of *coiled tubing* before they were used in wells.

Crack extension for every load displacement point was determined using the potential drop method. The differences between stable crack growth obtained by potential drop method and direct measurement on the tube fracture surface used as references were in all the cases smaller than 10%.

The *R* curves determined are only valid for current evaluated conditions because plain strain condition did not exist.

J-R curves showed a variation with the $2C_0/W$ ratio, probably by in plane constraint dependence.

J-R curves of coiled tubing with an initial crack location next to the weld, CTBs, seem to be higher than the *R* curves of coiled tubing with initial crack location opposite to the weld. Apparently, due to the longitudinal weld acted as a barrier for the crack arc growth.

The present work is a first step in the instability analysis of coiled tubing. On going work on this analysis is already in progress. Stability analysis of crack involves the determination of critical load at which the crack will grow in an unstable manner. This is being evaluated by carrying out elastic-plastic fracture mechanics (EPFM) analysis of coiled tubing with a through wall circumferential crack. From the *R* curves determined in this paper, the *J-integral* tearing modulus approach is being used for constructing the stability assessment diagram. For this purpose, Ainsworth [18] modified EPRI relationships are being used, taking into account that coiled tubing material—a low carbon steel—flow behavior deviates considerably from that given by a power law model [19,20].

Acknowledgment

The authors wish to acknowledge CONICET, San Antonio International and Universidad Nacional del Comahue (UNComa) for the helpful support.

References

[1] Quality Tubing NOV Procedures, http://www.nov.com/uploadedFiles/Business_Groups/Quality_Tubing/Coiled_Tubing_Products_and_Service/Coiled_-Tubing_Products/QTI%20procedures.pdf

Downloaded 09 May 2012 to 130.207.50.37. Redistribution subject to ASME license or copyright; see http://www.asme.org/terms/Terms_Use.cfm

[2] Tipton, S. M., 1996, "Multiaxial Plasticity and Fatigue Life Prediction in Coiled Tubing. Fatigue Life Time Predictive Techniques," ASTM STP 1292, Vol. 3, pp. 283–304.
[3] Tipton, S. M., 1998, "Low Cycle Fatigue Testing of Tubular Material Using Non-Standard Specimens. Effects of Product Quality and Design Criteria on Structural Integrity," ASTM STP 1337, pp. 102–119.
[4] ASTM E 1820-08, 2008, "Standard Test Method for Measurement of Fracture Toughness," American Society for Testing and Materials, Philadelphia.
[5] Chattopadhyay, J., Dutta, B. K., and Kushwaha, H. S., 2000, "Experimental and Analytical Study of Three Point Bend Specimen and Through Wall Circumferentially Cracked Straight Pipe," Int. J. Pressure Vessel Piping, **77**, pp. 455–471.
[6] Cerny, I., Knei, M., and Linhart, V., 1998, "Measurement of Crack Length and Profile in Thick Specimens and Components Using Modified DCPD Method," in *Proceedings of the 5th International Conference in Damage and Fracture Mechanics*, Bologna, Southampton, UK, June, Computational Mechanics Publications.
[7] Cerný, I., 2004, "The Use of DCPD Method for Measurement of Growth of Cracks in Large Components at Normal and Elevated Temperatures," Eng. Fract. Mech., **71**, pp. 837–848.
[8] Perez Ipiña, J. E., Mecánica de Fractura.-1aed.-2004, Buenos Aires: Librería y Editorial Alsina.
[9] Wilkowski, G. M., and Maxey, W. A., 1981, "Review and Applications of the Electric Potential Method for Measuring Crack Growth in Specimens, Flawed Pipes, and Pressure Vessels," ASTM STP 791, Fracture Mechanics: Fourteenth Symposium - Volume II: Testing and Applications, June 30–July 2, Los Angeles.
[10] Wilkowski, G. M., Guerrieri, D., Jones, D., Olson, R., and Scott, P., 1990, "Recent Results of Fracture Experiments on Carbon Steel Welded Pipes," Int. J. Pressure Vessels Piping, **43**(1–3), pp. 329–350.
[11] Chattopadhyay, J., Dutta, B. K., and Kushwaha, H. S., 2001, "Derivation of γ Parameter From Limit Load Expression of Crack Component to Evaluate *J-R* Curve," Int. J. Pressure Vessels Piping, **78**, pp. 401–427.
[12] Zahoor, A., and Kanninen, M. F., 1981, "A Plastic Fracture Mechanics Prediction of Instability in Circumferentially Cracked Pipe in Bending-Part 1: J-Integral Analysis," ASME J. Pressure Vessel Technol., **103**, pp. 352–358.
[13] Wilkoski, G. M., Zahoor, A., and Kanninen, M. F., 1981, "A Plastic Fracture Mechanics Prediction of Fracture Instability in a Circumferentially Cracked Pipe in Bending. Part II: Experimental Verification on a Type 304 Stainless Steel Pipe," ASME J. Pressure Vessel Technol., **103**, pp. 359–365.
[14] Zahoor, A., 1989, *Ductile Fracture Handbook,* Vol. 1, Novetech Corporation, Electric Power Research Institute in Rockville, MD, Palo Alto, California.
[15] Zhu, X. K., and Jang, S. K., 2001, "*J-R* Curves Corrected by Load-Independent Constraint Parameter in Ductile Crack Growth," Eng. Fract. Mech., **68**, pp. 285–301.
[16] Pavankumar, T. V., Chattopadhyay, J., Dutta, B. K., and Kushwaha, H. S., 2000, "Numerical Investigations of Crack Tip Constraint Parameters in Two Dimensional Geometries," Int. J. Pressure Vessels Piping, **77**, pp. 345–355.
[17] Heerens, J., Zerbst, U., and Schwalbe, K. H., 1993, "Strategy for Characterizing Fracture Toughness in the Ductile to Brittle Transition Regime," Fatigue Fract. Eng. Mater. Struct., **16**(11), pp. 1213–1230.
[18] Ainsworth, R. A., 1984, "The Assessments of Defects in Structures of Strain Hardening Materials," Eng. Fract. Mech., **19**, pp. 633–642.
[19] Anderson, T. L., 1995, *Fracture Mechanics, Fundamentals and Applications*, CRC, Ch. 9.
[20] Saxena, S., and Ramachandra Murthy, D. S., 2007, "On the Accuracy of Ductile Fracture Assessment of Through-Wall Cracked Pipes," Eng. Struct., **29**, pp. 789–801.

Downloaded 09 May 2012 to 130.207.50.37. Redistribution subject to ASME license or copyright; see http://www.asme.org/terms/Terms_Use.cfm